Ocean-Atmosphere-Land Interaction during the First Transition of Asian Summer Monsoon

許晃雄
國立台灣大學大氣科學系

Abstract

This study investigates the temporal and spatial variations of surface energy fluxes in South and Southeast Asia during the first transition of Asian summer monsoon. Vigorous ocean-atmosphere-land interaction is identified and is proposed to have an important impact on the abrupt changes in the large-scale circulation and convection during the transition.

1. Introduction

Hsu and Chen (1997), Terng and Hsu (1997) investigated the abrupt changes in large-scale circulation and convection during first transition of Asian Summer Monsoon (hereafter referred to as ASM). Their studies identified the close temporal relationship between the variations of the atmospheric circulation and surface temperatures. The major features include:

(1) Before the transition, the deep convection is located to the south of the warm ocean surface in the Bay of Bengal where the sea surface temperature (SST) is rising. During the transition, the deep convection moves abruptly northward to the Bay of Bengal where the SST starts to drop significantly.

(2) Before the transition, the deep convection between 10N-20N only occurs over the Indochina peninsula over the high terrain and warm land surface. The land surface continues dropping through the whole transitional period.

The above results suggest the ocean-atmosphere and atmosphere-land interaction in South and Southeast Asia may have crucial effects on the abrupt changes during the first transition.

This study is the continuation of the previous studies, by investigating the temporal variation and spatial distribution of surface energy fluxes. Real observations of related variables such as radiation and heat fluxes are not in existence. In this study, we analyze the re-analyses recently completed by ECMWF, NCEP, and NASA DAO to further our understanding in the effects of the ocean-atmosphere and atmosphere-land interactions. Other data such as optical depth, cloud amount in ISCCP and the OLR are also used to inter-compare and confirm the findings.

2. Inter-comparison of re-analyses

Re-analyses from different centers are strongly affected by the 4D data assimilation and numerical model. Therefore, it is necessary to investigate the discrepancies among the three analyses. Climatological means of various surface energy fluxes for the six sets of ten-day averages (4/30-5/09, 5/10-5/19, 5/20-5/29, 5/30-6/08, 6/09-6/18, and 6/19-6/28) derived from three re-analyses were inter-compared to understand the extent of the differences. The results of inter-comparison are:

(1) Temporal variations of surface fluxes are qualitatively similar in all three re-analyses, while they may differ significantly in magnitude for some particular variables.

(2) The largest discrepancy between re-analyses is found in short-wave radiation, while the latent and sensible heat fluxes are much more consistent between the re-analyses.

(3) Overall, good agreements are found in the Bay of Bengal, Indochina Peninsula, and Southern China, while poor agreements are observed in the South China Sea. The later is largely due to the short-wave radiation.

3. Results

The above inter-comparison indicates latent and sensible heat fluxes are the more reliable than radiation, especially in the crucial regions such as the Bay of Bengal, Indochina Peninsula. Since the atmosphere is heated mainly by latent and sensible heat fluxes, the result suggests that these two fluxes derived from re-analyses can be used for a qualitative study of the ocean-atmosphere-land interaction in South and Southeast Asia. To investigate the possible effects of heat fluxes, mean values for each pentad from pentad -6 to pentad 6 were calculated based on the transitional dates defined by Hsu and Chen (1997). Since the ECMWF daily re-analysis is not yet available to us, the following results are based on the NCEP and NASA re-analyses. Characteristics of the variations of various fluxes from pentad -6 to pentad 6 in several regions, based on NCEP re-analysis, are summarized as follows (Figure 1).

Bay of Bengal:

- Steady and significant increase of latent heat flux from 97 Wm^{-2} to 157 Wm^{-2}
- Slight decrease of sensible heat flux from 29 Wm^{-2} to 21 Wm^{-2}
- Steady increase of total flux from -44 Wm^{-2} to 12 Wm^{-2}

Indochina Peninsula:

- Steady but small increase of latent heat flux from 123 Wm^{-2} to 139 Wm^{-2}
- Slight decrease of sensible heat flux from 13 Wm^{-2} to -1 Wm^{-2}
- Steady increase of total flux from -12 Wm^{-2} to 0 Wm^{-2}

Northern SCS:

- Steady but small increase of latent heat flux from 60 Wm^{-2} to 80 Wm^{-2}
- Near-zero sensible heat flux
- Steady increase of total flux from -125 Wm^{-2} to -90 Wm^{-2}

Southern SCS:

- Steady but small increase of latent heat flux from 104 Wm^{-2} to 110 Wm^{-2}
- Near-zero sensible heat flux
- Steady increase of total flux from -35 Wm^{-2} to -25 Wm^{-2}

Southern China:

- Steady but small increase of latent heat flux from 112 Wm^{-2} to 126 Wm^{-2}
- Near-zero sensible heat flux
- Little change of total flux

4. Discussion

Ocean-atmosphere interaction: (Figures 2-3)

Before the transition, latent heat fluxes are small in the Arabian Sea, the Bay of Bengal, and the northern South China Sea. At the same time, short-wave radiation is large over the oceans where the convection is suppressed, consistent with the small cloud optical depth based on ISCCP data. After the transition, latent heat flux increases abruptly in the Arabian Sea and the Bay of Bengal due to the onset of the strong surface southwesterly, while short-wave radiation decreases and the cloud optical depth increases dramatically due to the cloudiness. Small latent heat flux and large short-wave radiation before the transition tend to heat the top oceanic surface, while large latent heat flux and small short-wave radiation would lead to the drop of the SST.

The large amount of the moisture released from the ocean fuels the convection both over the ocean and the land in the southern slope of the Tibetan Plateau. Latent heat released in the deep convection may intensify the low-level cyclonic circulation and the southwesterly which in turn can pump more moisture from the ocean.

Atmosphere-land interaction: (Figure 2-3)

Before the transition, both latent and sensible heat fluxes in the Indochina Peninsula are larger than those in the Bay of Bengal and the South China Sea. The combination of the surface heating and lifting effect of the high terrain would favor the occurrence of the deep convection in the region. This finding is consistent with the continuing decrease of the land surface temperature and the large diabatic heating release in the same area, as found by Hsu and Chen (1997). This suggests an interaction between the atmosphere and the land over the Indochina Peninsula.

It is proposed that the combined effect of the ocean-atmosphere interaction in the Bay of Bengal and the atmosphere-land interaction in the Indochina Peninsula may lead to the abrupt changes in the large-scale circulation and the convection.

5. References

Hsu, H.-H. and C.-T. Chen, 1997: Evolution of large-scale circulation and heating during the first transition of Asian summer monsoon. Submitted to J. Climate.

Terng, C.-T. and H.-H. Hsu, 1997: Fluctuations of circulation during the onset of Asian summer monsoon. Submitted to Atmospheric Sciences (in Chinese).

6. Figure caption

Figure 1. Area-means of diabatic heating, latent heat flux, sensible heat flux, short and short wave radiation, and total surface flux in different regions.

Figure 2. Surface latent heat flux on pentad -4, 0, and 4.

Figure 3. Surface total flux on pentad -4, 0, and 4.

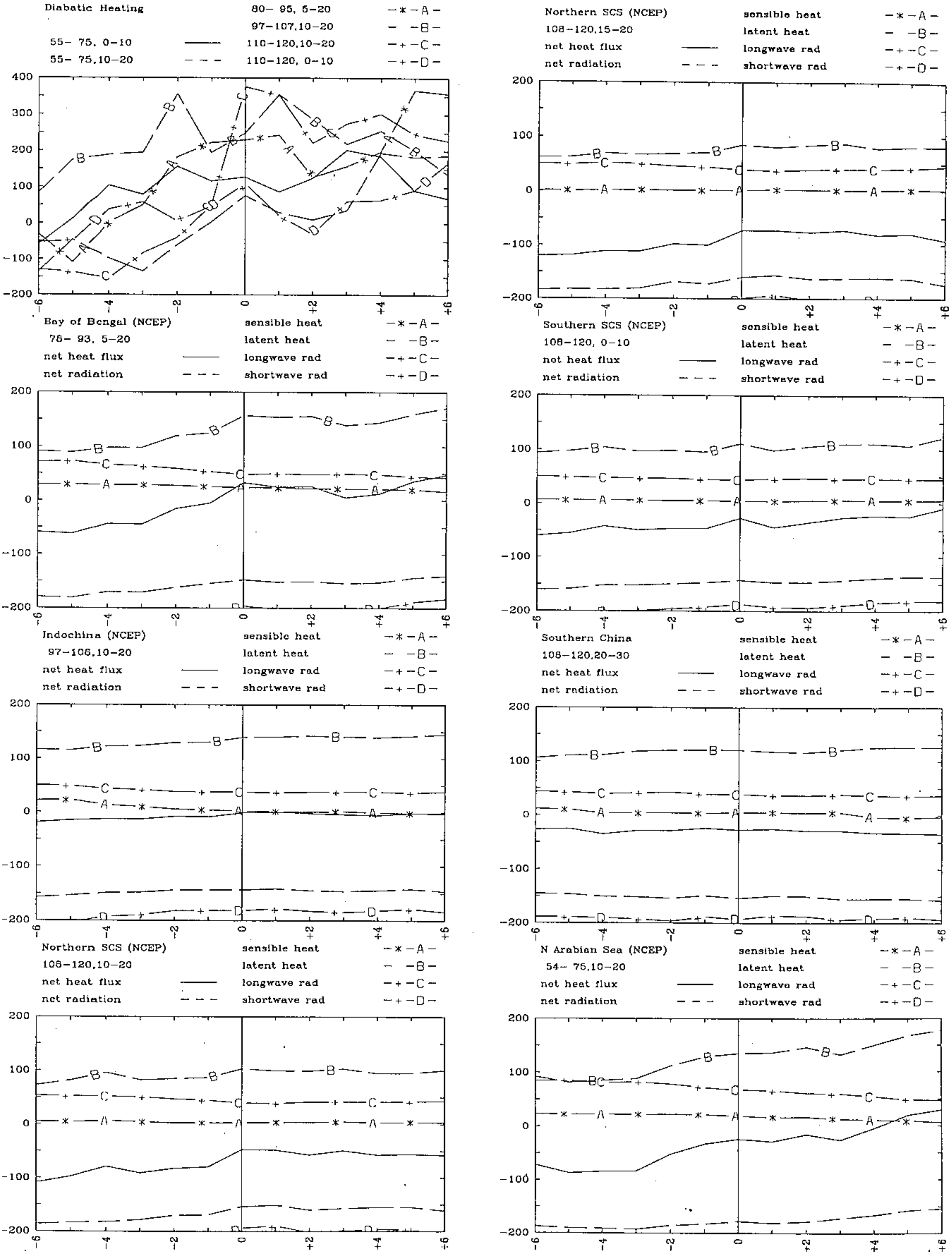
Diabatic Heating
55- 75, 0-10
55- 75,10-20
80- 95, 5-20 —*—A—
97-107,10-20 — —B—
110-120,10-20 —+—C—
110-120, 0-10 —+—D—
Northern SCS (NCEP)
108-120,15-20
net heat flux
net radiation
sensible heat —*—A—
latent heat — —B—
longwave rad —+—C—
shortwave rad —+—D—
Bay of Bengal (NCEP)
78- 93, 5-20
net heat flux
net radiation
sensible heat —*—A—
latent heat — —B—
longwave rad —+—C—
shortwave rad —+—D—
Southern SCS (NCEP)
108-120, 0-10
net heat flux
net radiation
sensible heat —*—A—
latent heat — —B—
longwave rad —+—C—
shortwave rad —+—D—
Indochina (NCEP)
97-106,10-20
net heat flux
net radiation
sensible heat —*—A—
latent heat — —B—
longwave rad —+—C—
shortwave rad —+—D—
Southern China
108-120,20-30
net heat flux
net radiation
sensible heat —*—A—
latent heat — —B—
longwave rad —+—C—
shortwave rad —+—D—
Northern SCS (NCEP)
108-120,10-20
net heat flux
net radiation
sensible heat —*—A—
latent heat — —B—
longwave rad —+—C—
shortwave rad —+—D—
N Arabian Sea (NCEP)
54- 75,10-20
net heat flux
net radiation
sensible heat —*—A—
latent heat — —B—
longwave rad —+—C—
shortwave rad —+—D—

Figure 1

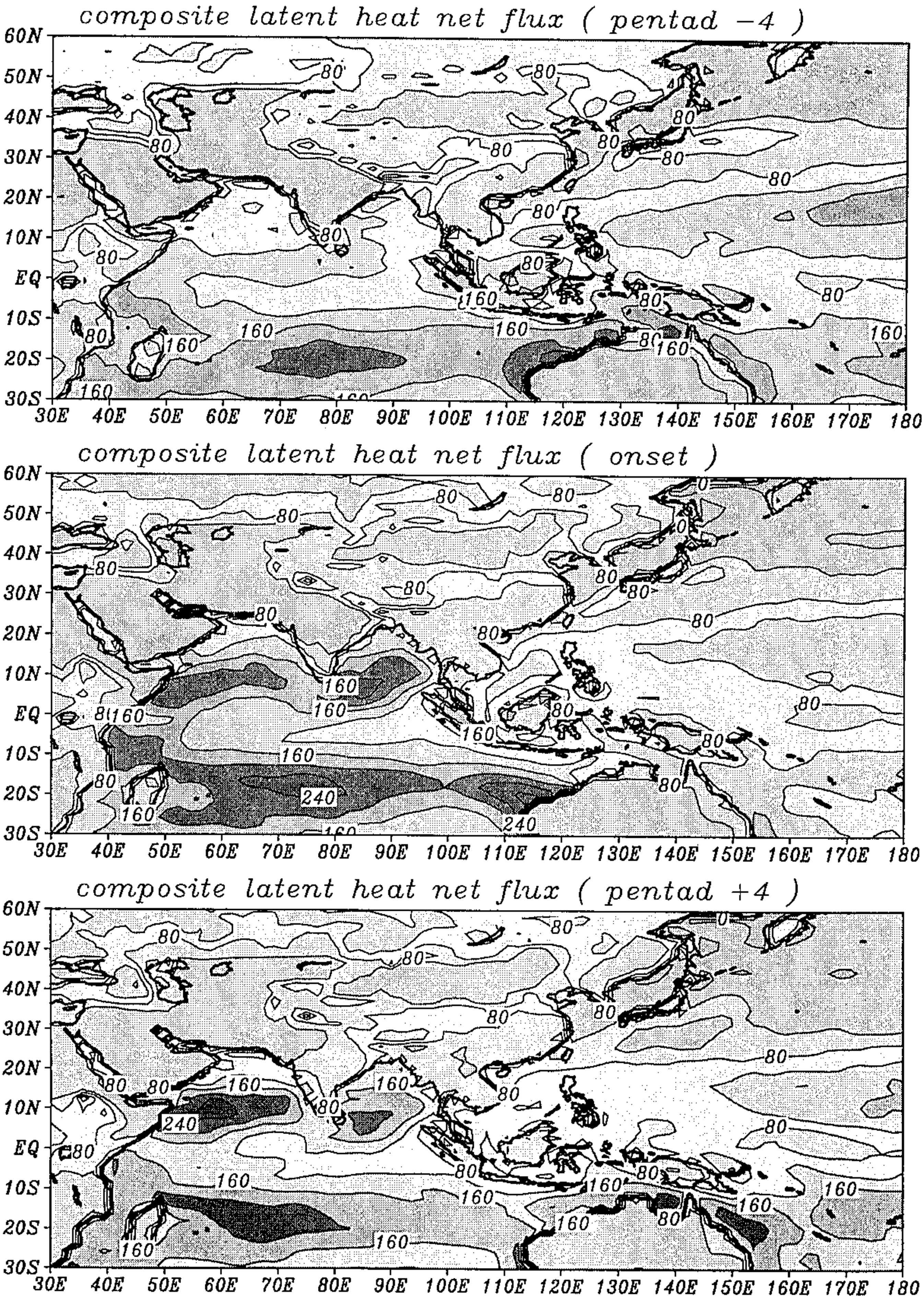
composite latent heat net flux (pentad −4)
composite latent heat net flux (onset)
composite latent heat net flux (pentad +4)
60N
50N
40N
30N
20N
10N
EQ
10S
20S
30S
30E
40E
50E
60E
70E
80E
90E
100E
110E
120E
130E
140E
150E
160E
170E
180

Figure 2

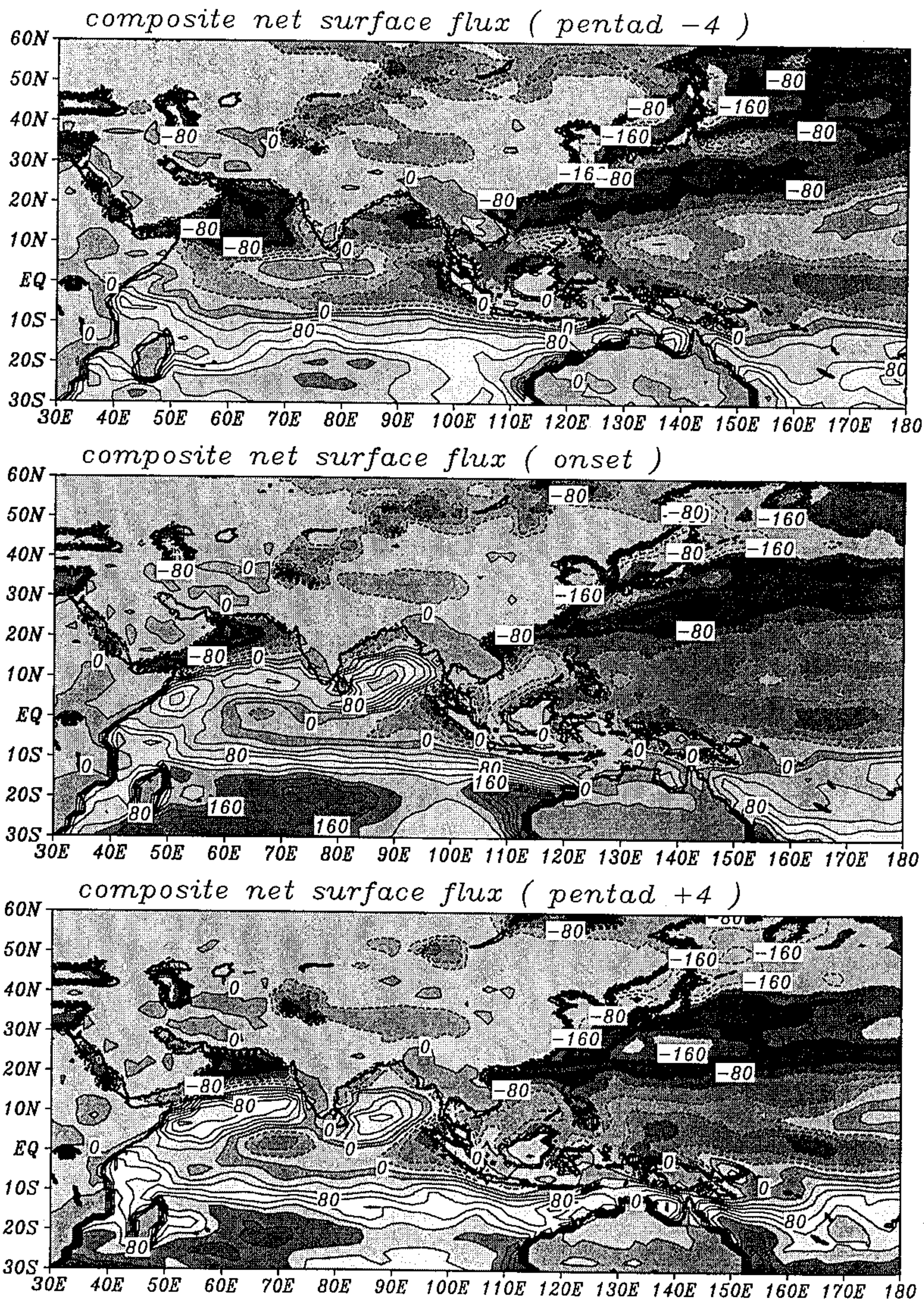
composite net surface flux (pentad −4)
composite net surface flux (onset)
composite net surface flux (pentad +4)
60N
50N
40N
30N
20N
10N
EQ
10S
20S
30S
30E
40E
50E
60E
70E
80E
90E
100E
110E
120E
130E
140E
150E
160E
170E
180

Figure 3